InSAR observations of the 2009 Racha earthquake, the Republic Georgia

E. Nikolaeva[1,2], T.R. Walter[1]

[1]Department 2- Physics of the Earth, Helmholtz Center Potsdam – GFZ German Research Center of Geosciences, Potsdam, Germany

now: [2]Ilia State University, Tbilisi, Georgia

corresponding e-mail: elenanikolaeva@hotmail.com

Abstract

Central Georgia is an area strongly affected by earthquake and landslide hazards. On 29th April 1991 a major earthquake (Mw=7.0) struck the Racha region in the republic Georgia, followed by aftershocks and significant afterslip. The same region was hit by another major event (Mw=6.0) on 7th September 2009. The aim of the study reported here was to utilize geodetic data as synthetic aperture radar interferometry (InSAR) to improve a knowledge about the spatial pattern of deformation due to the earthquakes in the seismic active central Georgia. There were no actual earthquake observations by InSAR in Georgia.

We considered all available SAR data images from different space agencies. However, due to the long bandwith and the frequent acquisitions, only the multi-temporal ALOS L-band SAR data allowed us to produce interferograms spanning the 2009 earthquake. ~~We used the multi-temporal ALOS L-band InSAR data to produce interferograms spanning times before and after the 2009 earthquake.~~ We detected a local uplift around 10 cm in the interferogram near the earthquake's epicenter whereas evidence of surface ruptures could not be found in the field along the active thrust fault. We simulated a deformation signal which could be created by the 2009 Racha earthquake on the basis of local seismic records and by using an elastic dislocation model. ~~The observed InSAR deformation is in good agreement with our model~~. We compared our modeled fault surface of the September 2009 with the April 1991 Racha earthquake fault surfaces, and identify the same fault or a sub-parallel fault of the same system as the origin. The patch that was active in 2009 is just adjacent to the 1991 patch,

indicating a possible mainly westward propagation direction, with important implications for future earthquake hazards.

1. Introduction

Large tectonic earthquakes often occur in spatial and temporal proximity. In some cases, these earthquakes successively rupture the same fault with a well-defined propagation direction (Lin and Stein 2004; Burgmann et al. 2000). As seen in the North Anatolian fault (Pondard et al. 2007; Stein, Barka, and Dieterich 1997) or in the San Andreas fault (Lin and Stein 2004), these propagation directions allow for assessment of seismic hazard potential.

One geologically active environment, with numerous damaging earthquakes and landslide hazards occurring during the 20th century, lies in the Republic of Georgia, specifically the Racha region. Triep et al. hypothesized that the Racha ridge region (the Greater Caucasus mountains) is a consequence of repeated earthquakes (Triep and Abets 1995). On 29th April 1991, a major earthquake (Mw=7.0) occurred along a blind thrust fault, causing severe damage to infrastructure and triggering other hazards, such as landslides and rock falls (Arefiev et al. 2006; R W Jibson et al. 1994). On 7th September 2009, a smaller earthquake (Mw=6.0) occurred in the same region. No clear rupture was observed except small cracks on the road and local small rock and land slid events. For instance, a landslide in the Sachkhere region showed a small, but relevant acceleration that might be associated with this earthquake (Nikolaeva et al. 2013).

Interferometric synthetic aperture radar (InSAR) has been widely used to measure tectonic deformations since the first publication comprehensively applied this method for the Landers earthquake in California (Massonnet et al. 1993). However, the focus has been on the earthquakes with magnitudes much greater than 6, which produce larger deformations (Wang et al. 2004; Funning 2005; R. E. Reilinger et al. 2000). In this case, the InSAR observations often show clear signals. The cases of small earthquakes are less studied because surface displacements are likely to be insignificant, uncertainties from satellite orbits and/or intervening atmospheric conditions (Bell, Amelung, and Henry 2012). However, several papers show that the InSAR can detect surface deformations in the case of shallow events with magnitudes smaller than 4.8 (Dawson and Tregoning 2007; Bell, Amelung, and Henry 2012).

In this study we used data from the ALOS L-band radar satellite to detect the coseismic surface deformation associated with the earthquake of the moment magnitude Mw=6.0 on 7th September 2009 in the Racha region. Specially, the aims of this paper are to investigate the ability of InSAR to provide the spatial pattern of deformation due to the 2009 Racha earthquake, to compare observations of geodetic data with a model based on local information about the earthquake and to find a link between the 1991 and 2009 earthquakes.

2. Study area

Located at the junction between the Arabian and Eurasian plates, the Caucasus is one of the most seismically active regions in the Alpine-Himalayan collision belt. Georgia, as part of the Caucasus, is located in the central faulted segment (Fig. 1), and has experienced both historical and recent strong earthquakes.

The study area belongs to a fold and thrust mountain belt of the Greater Caucasus (Adamia et al. 2010) with shallow northward dipping faults (Tan and Taymaz 2006). Consequently, the tectonics are represented mainly by vertical movements (Lilienberg 1980) as evidenced by the topography (Philip et al. 1989). The geological structure resulting from the tectonic movements represents the thrust-nappe system of the Greater Caucasus Range (Triep et al. 1995). The nappe system is formed by Cretaceous to Quaternary sediments and locally masks fault truces (Philip et al. 1989).

The analysis of the historical and instrumental seismological record shows that this region is of moderate seismicity (Balassanian et al. 1999). The possibility of extending the catalogue of strong events (instrumental records) until the beginning of 20th century is important for the seismic study of the region (van Westen et al. 2012). GPS measurements have shown that the Caucasus block moves at 13 mm/yr in an east-south direction relative to Eurasia and also has a rotational displacement component with respect to Eurasia (Reilinger et al., 2006).

In addition to the seismic activity, the complicated lithological-tectonic composition of the region and strong topographic reliefs underlines the relevance of exogenic processes, such as rainfall and erosion, accompanied by numerous landslides of different scales (Gracheva & Golyeva, 2010; Jibson, Randall, & Prentice, 1991; Nikolaeva et al., 2013).

2.1. The Racha earthquake 1991

One of the more powerful recorded earthquakes (M_s=7.0) occurred at 9:12 GMT (+5 hours local time) on 29th April 1991 in the Great Caucasus Range, Georgia, Racha region (Fuenzalida et al. 1997). There was no observed tectonic surface rupture associated with this earthquake, however dozens of fatalities occurred due to the landslides triggered by this event (Jibson et al., 1991). A series of aftershocks followed the main shock spanning several months. There were several significant aftershocks with a few tens of kilometers from the main shock (see Table 1). Several authors indicated four aftershock clusters (Triep and Abets 1995; Fuenzalida et al. 1997). Two clusters are located to the west one north and the second south of the Racha ridge (Fig. 1). The cluster in the east represents a distribution of mostly aftershocks of the June 15 event. The middle cluster shows the eastern part of the main aftershock area (Fig. 1).

The focal mechanism solution was obtained from the Harvard centroid moment tensor and corresponding to a pure thrust fault dipping to the north (strike=288^0, dip=39^0, rake=106^0). Later, the source parameters were extracted from teleseismic body- wave inversion for the meaningful aftershocks and showed thrust mechanisms on roughly E-W-oriented planes for main shock. However, the cluster in the east shows a trust fault N-S-oriented (Fuenzalida et al. 1997).

2.2. The Racha earthquake 2009

On 7th September 2009 at 22:41 GMT (+5 hours local time), an earthquake with a moment magnitude Mw=6.0 occurred in northern Georgia at a depth of 13.4 km (Fig. 1). The main shock epicenter was located ~80 kilometers north-east of the city of Kutaisi in the Oni district of the Racha-Lechkhumi region. The main shock was felt in Tbilisi (155 km south-east of the event), the capital of Georgia, and in the west of Georgia (Gori and Zugdidi towns). There were no reports of human losses. However, the tremors damaged at least 200 buildings, with some roads blocked by rock falls and subsequent damage to service lines (information from the Seismic Monitoring Center in Tbilisi, www.seismo.ge).

Within minutes, four aftershocks occurred with magnitudes greater than 4. More aftershocks followed later, with some reaching magnitudes greater than 4 until 13th

September 2009. The distribution of aftershocks has same orientation as one of the clusters of the 1991 Racha earthquake (Fig. 1).

Focal mechanism solutions were obtained from the arrival of P-waves with only minor variations in the avaliable solutions (Fuenzalida et al. 1997; Vakarchuk et al. 2013). We gathered all available data to form a characterization of the earthquake mechanism. The type of motion was consistently defined as being thrust, roughly dipping to the northeast (Triep and Abets 1995). Parameters from the Centroid Moment Tensor (CMT) solution are strike=314°, dip=28°, slip=106°, with the moment tensor solution showing a pure thrust mechanism without a strike slip component. Also, the focal mechanism solutions and the tectonic structure for the earthquake are available from the EMME (Earthquake Model of the Middle East Region, www.emme-gem.org), CMT (www.globalcmt.org) and Geophysical Survey, Russian Academy of Sciences (www.ceme.gsras.ru) websites.

3. Data and methods

We combined radar images of the Racha region acquired at different times to obtain the two pass interferometric phase. The interferometric phase contains information about the difference between two independent time measurements of the radar-to ground range (Hanssen 2001). In fact, there are very few SAR acquisitions for this area of central Georgia and for the studied time period (2008-2010) available in the European Space Agency archive, not allowing a detailed deformation study. There are no ERS data available at all. Envisat ASAR IM data are available for the date 2009-09-06 and 2009-11-15 (same track 178). However, these scenes only partly cover the area investigated. Envisat_ASAR_WS data are available from different tracks. Also, a coherence of these scenes is low due to the sensitivity of the C-band to the vegetation. Therefore we concentrate on the Japanese mission ALOS PALSAR, and here use all available data. Only the ascending track (eastward-viewing) of the ALOS satellite, the PALSAR L-band, is available for this area. Therefore one line-of-sight (LOS) component of the deformation field is observable.

We created eight interferograms by using SAR images. Four of the interferograms covered the pre-seismic period, three interferograms covered the co-seismic period, and only one covered the post-seismic. We formed single-look interferograms using the DORIS processing package (Kampes and Usai 1999). ~~The Shuttle Radar Topography Mission Digital Elevation Model (SRTM DEM) at 90 m resolution was subtracted from~~

~~each of the interferograms.~~ The phase component associated with the topography was removed from the interferograms, considering the Shuttle Radar Topography Mission Digital Elevation Model (SRTM DEM) at 90 m resolution.

To improve the quality of these interferograms, we applied a multilooking filtering approach, so that each pixel of an interferogram represents ~200 by square meters on the ground. The adaptive filter was used to smooth the speckles in the interferograms (Principe, De Vries, and De Oliveira 1993). We then used a two-dimensional phase unwrapping algorithm SNAPHU (Chen and Zebker 2001; Chen and Zebker 2002) to obtain unambiguous phase data. To remove the orbital contribution in the phase, we applied a wavelet multi-resolution analysis and robust regression (Shirzaei and Walter 2011). Atmospheric delay was extracted using the phase-elevation ratio (Zebker, Rosen, and Hensley 1997). In doing so, we considered the phase-elevation correlation in the south of the image far enough from the earthquake zone. After these corrections and filtering procedures were applied, we observed some relevant signals that reflect a deformation field. Further evaluation of this deformation field was made in comparison with the dislocation model described below.

3.1. Modeling

We used a dislocation model in elastic half space (Okada 1985) to extract the possible deformation pattern due to the 2009 Racha earthquake. The model calculates the displacement arising from a defined fault plane position and geometry. The model considers the geometry of the fault plane (length and width), the position of the fault in space (strike, depth, dip, coordinates of upper middle edge of fault) and the displacement components (strike-slip and dip-slip).

We utilized the strike and dip from the above presented average focal mechanism solution. Other parameters were calculated based on the known moment magnitude and epicenter of the earthquake. For the first approximation, we assumed that the fault size was 10 by 10 km (Donald, Coppersmith, and Coppersmith 1994). Assuming the moment magnitude (M_w) of 6.0, we can estimate an average displacement (*D)* of 0.33 meters, with a rigidity constant ($3*10^{11}$ dyne/cm^2) and the seismic moment from the formula of Hanks and Kanamori (Hanks and Kanamori 1979).

4. Results

4.1. InSAR

All pre-seismic interferograms lack significant deformation in the Racha region (Fig. 2 (a-d)). This inactivity is confirmed by three different interferograms Three co-seismic interferograms, in turn, show a deformation signal around the fault zone area with consistent scale (Fig. ~~3~~ 2 (e-g)). The deformation field is elongated NW-SE and occurs in the region of the aftershocks following the 2009 event. The long axis is about 15 km, parallel to the seismogenic fault constrained earlier (Gamkrelidze and Shengelia 2007). The maximum value of deformation reached is 10 centimeters in the line-of-sight. The deformation is mostly due to uplift in the region north of the alleged fault (Fig. 1). The interferogram 20090904-20091020 (yyyymmdd) is built from acquisitions 4 days before the earthquake and 42 days after (Fig. 2(f)). This interferogram has a good quality (coherence is higher than 0.7) and it includes the phase changes associated with main event and significant aftershocks (Table 1). The other small aftershocks (M<4.5) did not contribute to the deformation signal based on InSAR analysis (Dawson and Tregoning 2007). The observed deformation by InSAR has a good correlation with the distribution of aftershocks. We note that the three co-seismic interferograms all use the same slave image. Building independent interferograms was not feasible because of limited high quality data in the archive for the central Georgia.

One post-seismic interferogram has a slightly poor quality (coherence is low than 0.4) (Fig. 2 (h)). However, it shows no clear deformation signal.

4.2. Okada model

Our initial dislocation elastic half-space model is based on the main event focal mechanism, CMT solution: strike=314^0 and dip=28^0 (Fig. 3(a)). The dip slip of 0.33 m is based on the assumption that the fault is a rectangle and has the parameters length=10 km, width=10 km. The depth (10 km) and position is in the middle of the fault plane and was calculated based on knowledge of the earthquake‘s epicenter. The model generally reproduces the distribution of deformation, as shown by the residuals when subtracted from the InSAR data (Fig. 3 (a)).

The shallowest edge of the fault, however, is not identical to the main orientation of the deformation from the InSAR observations in modeling case (Fig. 3 (a)). We found that the modeled deformation of a fault oriented 288^0 from north clockwise better fits the deformation observed in the InSAR results. This trend is also in agreement with the

1991 Racha earthquake, as will be further discussed below. To understand the mechanism of the fault, we had to consider the rupture geometry within the context of previous earthquakes.

5. Discussion

Using satellite radar interferometry, we investigated the displacement associated with the 2009 Racha earthquake. We assessed the ALOS radar data catalogue and processed data that covered the earthquake area and the times around the event. The distribution of deformation and aftershocks of the 2009 earthquake have a good correlation with one of the aftershock clusters of the 1991 earthquakes. How might these two events be related?

A comparison of the epicenters from the 1991 and 2009 events reveal the same latitude and a difference of only 0.1^0 in longitude (the local catalog data). Also, as we described before, the deformation InSAR trench is well fit by a model with a strike $=288^0$ (Fig.3 (b)). This strike presents the Harvard CMT solution for the 1991 Racha earthquake (Fuenzalida et al. 1997). Therefore, the interesting question is if the 2009 earthquake occurred on exactly the same fault as the 1991 earthquake and, if so, did the 2009 earthquake fill a seismogenic gap? Answering this question is challenging, because of the complexity in the rupture geometries and dynamics of these events (Fuenzalida et al. 1997; Vakarchuk et al. 2013).

The fault system for the 1991 Racha earthquake was formed by four subsources using body wave inversion (Fuenzalida et al. 1997). One subsource significantly dominates the others. Therefore, the model presents a simple single rupture pattern. Based on observations of separate clusters of aftershocks (Arefiev et al. 2006), a model with three complex subsources was created (Vakarchuk et al. 2013). Two subsources represent a thrust type of motion. The reverse type of motion was hypothesized for one of the other subsources. Due to this complexity, it is possible that the use of a simple model does not fit well with the true fault.

The best-fit model determined by InSAR suggests the strike is 288^0 instead 314^0 (CMT), which could be explained by control of local structures. Also, based on the Harvard CMT solution, the dip of the fault might be steeper close to the surface, which was also confirmed by InSAR observation~~based on InSAR data, we can assume that the fault plane may be shallower to the surface~~. Vakarchuk et al. (2013) propose a hypo central depth of the 2009 earthquake of 7 kilometers instead of 15, according to CMT catalog (Vakarchuk et al. 2013). Although a surface rupture was not observed (Arefiev et al. 2006), a large number of landslides occured during and after the Racha 1991 earthquake (R.W. Jibson, Randall, and Prentice 1991). The distribution of the strongest co-seismic deformations in the Racha earthquake 1991 area (Arefiev et al. 2006; R W Jibson et al. 1994) is similar to the observed InSAR coseismic deformations associated with the Racha 2009 earthquake. In addition, the 2009 Racha earthquake triggered landslide activity (Nikolaeva et al. 2013). Consequently, the observed co-seismic deformation likely presents the cumulative effects of the landslides.

The comparison of possible faults for the earthquakes from the 1991 and 2009 (Fig. 4) might imply that the earthquakes are migrating to the north-west. The fault rupture of the earthquake 2009 may belong to the same fault system that was active in 1991.

Limitations of the herein discussed results mainly may come from the quality and quantity of the InSAR data. Only one viewing component was available, and a small amount of radar data has been archived by the space agency. Therefore all co-seismic interferograms use the same slave image. Possibly this one image contributes noise and/or artifact components, which is then present in all generated interferograms. However, the same slave image is used in post-seismic interferograms, which do not show this deformation pattern. Despite this, the presented InSAR results allow us to develop a general concept about the displacement occurrence and are the only geodetic source available for the studied event.

6. Conclusion

The central region of the Republic of Georgia repeatedly suffers from earthquakes and landslides. Here, we investigated the recent 2009 Racha earthquake by applying the InSAR method and modeling. We used the multi-temporal ALOS satellite L-band radar images, acquired in ascending mode for the period before, during and after the earthquake. We generated two-pass interferograms and after filtering could identify a significant signal that likely reflects the coseismic displacement field. The observed InSAR ground deformation is around 10 cm in LOS and probably comes from the cumulative effects of the main shock, aftershocks and triggering events. The deformation model of the 2009 Racha earthquake is in a good agreement with the observed InSAR deformation signal. Results suggest that the 2009 Racha earthquake (Mw=6.0) occurred on the same or sub-parallel fault as the 1991 event. A high spatial resolution of the InSAR data allows to track a distribution of deformation due to the earthquake in the region which is difficult of access as high mountain Racha.

Our research demonstrates the ability of the InSAR L-band to observe deformations arising from small tectonic events and provides new insights into the tectonic processes of the Caucasus based on radar remote sensing data. Nowadays with the availability of modern satellites and background missions (e.g. Sentinel), the availability of data for future earthquakes will certainly be improved. Further, InSAR data has the potential to allow us to learn more about the rupture process of earthquakes in the years after the initial event. The main deformations were rock avalanches and landslides for both earthquakes. Thus, the mapping of the deformation zone after an earthquake reveals the distribution density of landslides in the Racha area.

Acknowledgments

The authors are grateful to Onur Tan for providing a slip distribution of the 1991 Racha earthquake and discussion. Also we would like to acknowledge Alessandro Parizzi and Hannes Bathke for examination of our interferograms.

References

Adamia, S., V. Alania, A. Chabukiani, G. Chichua, O. Enukidze, and N. Sadradze. 2010. “Evolution of the Late Cenozoic Basins of Georgia (SW Caucasus): A Review.” *Geological Society, London, Special Publications* 340 (1): 239–59. doi:10.1144/SP340.11.

Arefiev, S. S., E. A. Rogozhin, V. V. Bykova, and C. Dorbath. 2006. “Deep Structure of the Racha Earthquake Source Zone from Seismic Tomography Data.” *Izvestiya, Physics of the Solid Earth* 42 (1): 27–40. doi:10.1134/S1069351306010034.

Balassanian, S., T. Ashirov, T. Chelidze, A. Gassanov, N. Kondorskaya, and G. Molchan. 1999. “Seismic Hazard Assessment for the Caucasus Test Area.” *ANNALI DI GEOFISICA* 42 (6): 1139–51.

Bell, John W., Falk Amelung, and Christopher D. Henry. 2012. “InSAR Analysis of the 2008 Reno-Mogul Earthquake Swarm: Evidence for Westward Migration of Walker Lane Style Dextral Faulting.” *Geophysical Research Letters* 39 (18): n/a–n/a. doi:10.1029/2012GL052795.

Burgmann, R., D. Schmidt, R.M. Nadeau, M. d’Alessio, E. Fielding, D. Manaker, T.V. McEvilly, and M.H. Murray. 2000. “Earthquake Potential Along the Northern Hayward Fault , California.” *Science* 289 (August): 1178–83.

Chen, C.W., and H. A. Zebker. 2001. “Two-Dimensional Phase Unwrapping with Use of Statistical Models for Cost Functions in Nonlinear Optimization.” *Journal of the Optical Society of America* 18: 338–51.

Chen, C.W., and H.A. Zebker. 2002. “Phase Unwrapping for Large SAR Interferograms: Statistical Segmentation and Generalized Network Models.” *IEEE Transactions on Geoscience and Remote Sensing* 40: 1709–19.

Dawson, John, and Paul Tregoning. 2007. “Uncertainty Analysis of Earthquake Source Parameters Determined from InSAR : A Simulation Study.” *Journal of Geophysical Research* 112: 1–13. doi:10.1029/2007JB005209.

Donald, L, W.J. Coppersmith, and K.J. Coppersmith. 1994. “New Empirical Relationships among Magnitude , Rupture Length , Rupture Width , Rupture Area , and Surface Displacement.” *Bulletin of the Seismological Society of America* 84 (4): 974–1002.

Fuenzalida, H., L. Rivera, H. Haessler, D. Legrand, H. Philip, L. Dorbath, D. McCormack, S. Arefiev, C. Langer, and A. Cisternas. 1997. “Seismic Source Study of the Racha-Dzhava (Georgia) Earthquake from Aftershocks and Broad-Band Teleseismic Body-Wave Records: An Example of Active Nappe Tectonics.” *Geophysical Journal International* 130 (1): 29–46. doi:10.1111/j.1365-246X.1997.tb00985.x.

Funning, Gareth J. 2005. “Surface Displacements and Source Parameters of the 2003 Bam (Iran) Earthquake from Envisat Advanced Synthetic Aperture Radar Imagery.” *Journal of Geophysical Research* 110 (B9): B09406. doi:10.1029/2004JB003338.

Gracheva, Raisa, and Alexandra Golyeva. 2010. “Landslides in Mountain Regions: Hazards, Resources and Information.” In *Geophysical Hazards, International Year of Planet Earth*, edited by Tom Beer, 249–60. Dordrecht: Springer Netherlands. http://www.springerlink.com/index/10.1007/978-90-481-3236-2.

Hanks, Thomas C., and Hiroo Kanamori. 1979. “A Moment Magnitude Scale.” *Journal of Geophysical Research* 84 (B5): 2348. doi:10.1029/JB084iB05p02348.

Hanssen, R F. 2001. *Radar Interferometry: Data Interpretation and Error Analysis*. Kluwer Academic Publishers, Dordrecht.

Jibson, R W, C S Prentice, B A Borissoff, E A Rogozhin, and C J Langer. 1994. “Some Observations of Landslides Triggered by the 29 April 1991 Racha Earthquake, Republic of Georgia.” *Bulletin Seismological Society of America* 84 (4): 963–73. http://www.scopus.com/inward/record.url?eid=2-s2.0-0028667427&partnerID=40&md5=ab8f839699fc3eacbd45a3f1854a8530.

Jibson, R.W., W. Randall, and Carol S. Prentice. 1991. “Ground Failure Produced by the 29 April 1991 Racha Earthquake in Soviet Georgia.” *U.S. Geological Survey*, 10. http://books.google.de/books/about/Ground_Failure_Produced_by_the_29_April.html?id=xNYsYgEACAAJ&redir_esc=y.

Kampes, B, and S Usai. 1999. “Doris: The Delft Object-Oriented Radar Interferometric Software.” In *2nd International Symposium on Operationalization of Remote Sensing Enschede The Netherlands*. doi:10.1.1.46.1689.

Lin, Jian, and Ross S Stein. 2004. “Stress Triggering in Thrust and Subduction Earthquakes and Stress Interaction between the Southern San Andreas and Nearby Thrust and Strike-Slip Faults.” *Journal of Geophysical Research* 109: 1–19. doi:10.1029/2003JB002607.

Massonnet, Didier, Marc Rossi, César Carmona, Frédéric Adragna, Gilles Peltzer, Kurt Feigl, and Thierry Rabaute. 1993. “The Displacement Field of the Landers Earthquake Mapped by Radar Interferometry.” *Nature* 364 (6433): 138–42. doi:10.1038/364138a0.

Nikolaeva, E., T. R. Walter, M. Shirzaei, and J. Zschau. 2013. “Landslide Dynamics and Coupling Revealed by L-Band InSAR in Central Georgia.” *Natural Hazards and Earth System Sciences Discussions* 1 (5): 4925–62. doi:10.5194/nhessd-1-4925-2013.

Okada, Y. 1985. “Surface Deformation due to Shear and Tensile Faults in a Half-Space.” *International Journal of Rock Mechanics and Mining Sciences Geomechanics Abstracts* 75 (4). Seismological Society of America: 1135–54. doi:10.1016/0148-9062(86)90674-1.

Philip, H., A. Cisternas, A. Gvishiani, and A. Gorshkov. 1989. “The Caucasus: An Actual Example of the Initial Stages of Continental Collision.” *Tectonophysics* 161 (1-2): 1–21. doi:10.1016/0040-1951(89)90297-7.

Pondard, Nicolas, Rolando Armijo, Geoffrey C P King, and Bertrand Meyer. 2007. “Fault Interactions in the Sea of Marmara Pull-Apart (North Anatolian Fault): Earthquake Clustering and Propagating Earthquake Sequences.” *Geophysical Journal International*, 1185–97. doi:10.1111/j.1365-246X.2007.03580.x.

Principe, J. C., B. De Vries, and P. G. De Oliveira. 1993. “The Gamma-Filter-a New Class of Adaptive IIR Filters with Restricted Feedback.” *Signal Processing, IEEE Transactions on* 41 (2): 649–56.

Reilinger, R.E., S. Ergintav, R. Bürgmann, S. McClusky, O. Lenk, A. Barka, O. Gurkan, et al. 2000. “Coseismic and Postseismic Fault Slip for the 17 August 1999, M=7.5, Izmit, Turkey.” *Earthquake Science* 289: 1519–24.

Reilinger, Robert, Simon McClusky, Philippe Vernant, Shawn Lawrence, Semih Ergintav, Rahsan Cakmak, Haluk Ozener, et al. 2006. “GPS Constraints on Continental Deformation in the Africa-Arabia-Eurasia Continental Collision Zone and Implications for the Dynamics of Plate Interactions.” *Journal of Geophysical Research* 111 (B5). {AMER GEOPHYSICAL UNION}: 1–26. doi:10.1029/2005JB004051.

Shirzaei, Manoochehr, and Thomas R Walter. 2011. “Estimating the Effect of Satellite Orbital Error Using Wavelet-Based Robust Regression Applied to InSAR Deformation Data.” *IEEE Transactions on Geoscience and Remote Sensing* 49 (11): 4600–4605. http://ieeexplore.ieee.org/xpls/abs_all.jsp?arnumber=5779729.

Stein, Ross S, Aykut A Barka, and James H Dieterich. 1997. “Earthquake Stress Triggering.” *Geophysical Journal International*, 594–604.

Tan, O., and T. Taymaz. 2006. “Active Tectonics of the Caucasus: Earthquake Source Mechanisms and Rupture Histories Obtained from Inversion of Teleseismic Body Waveforms.” *Geological Society of America Special Papers* 409: 531–78. doi:10.1130/2006.2409(25).

Triep, E G, G A Abers, A L Lerner-Lam, V Mishatkin, N Zakharchenko, and O Starovoit. 1995. “Active Thrust Front of the Greater Caucasus: The April 29, 1991, Racha Earthquake Sequence and Its Tectonic Implications.” *Journal of Geophysical Research* 100 (B3): 4011–33. http://www.agu.org/pubs/crossref/1995/94JB02597.shtml.

Triep, E G, and G A Abets. 1995. “The April 29 , 1991 , Racha Earthquake Sequence and Its Tectonic Implications.” *Journal of Geophysical Research* 100 (94): 4011–33.

Vakarchuk, R. N., R. E. Tatevossian, Zh. Ya. Aptekman, and V. V. Bykova. 2013. “The 1991 Racha Earthquake, Caucasus: Multiple Source Model with Compensative Type of Motion.” *Izvestiya, Physics of the Solid Earth* 49 (5): 653–59. doi:10.1134/S1069351313050121.

Van Westen, C J, M W Straatsma, U D Turdukulov, W F Feringa, K Sijmons, K Bakhtadze, T Janelidze, N Kheladze, and [et al.]. 2012. *Atlas of Natural Hazards and Risk in Georgia*. Edited by C J van Westen. CENN Caucasus Environmental NGO Network.

Wang, R., Y. Xia, H. Grosser, H.-U. Wetzel, H. Kaufmann, and J. Zschau. 2004. “The 2003 Bam (SE Iran) Earthquake: Precise Source Parameters from Satellite Radar Interferometry.” *Geophysical Journal International* 159 (3): 917–22. doi:10.1111/j.1365-246X.2004.02476.x.

Zebker, Howard A., Paul A. Rosen, and Scott Hensley. 1997. “Atmospheric Effects in Interferometric Synthetic Aperture Radar Surface Deformation and Topographic Maps.” *Geophysical Research* 102: 7547–63. http://192.102.233.13/journals/jb/v102/iB04/96JB03804/96JB03804.pdf.

Table 1. Data from Global CMT catalog

Date	Lat	Lon	Mw	Strike	Dip	Slip
29.4.1991	42.6	43.61	6.9	288/87	39/53	106/77
29.4.1991	42.38	43.75	6.1	261/62	41/50	104/78
3.5.1991	42.54	42.94	5.6	315/87	47/55	127/57
15.6.1991	42.58	43.07	6.2	138/16	49/58	44/130

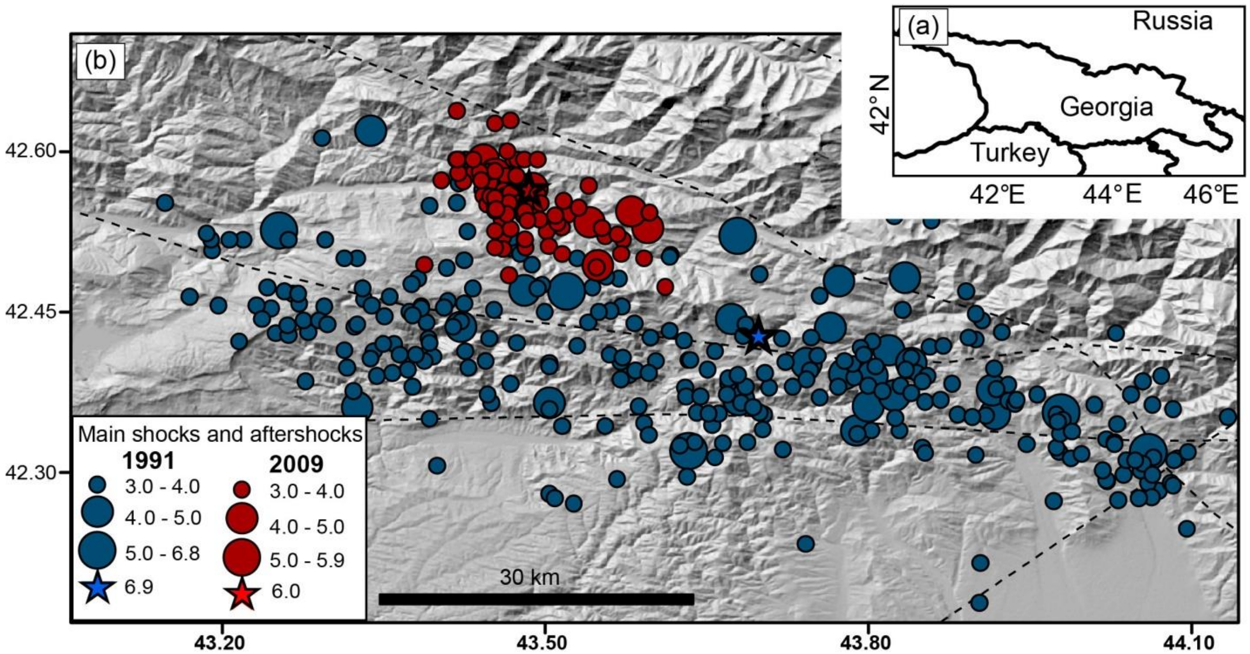

Figure 1. a) Location of the republic of Georgia. b) Distribution of locations of the Racha main shocks (stars) and aftershocks from 1991 (dark blue dots) and 2009 (dark red dots) with magnitudes greater than 4 (source: the catalog of the Seismic Monitoring Center (SMC) in Georgia, www.seismo.ge). Major faults are shown by black dashed lines (Gamkrelidze & Shengelia, 2007).

428

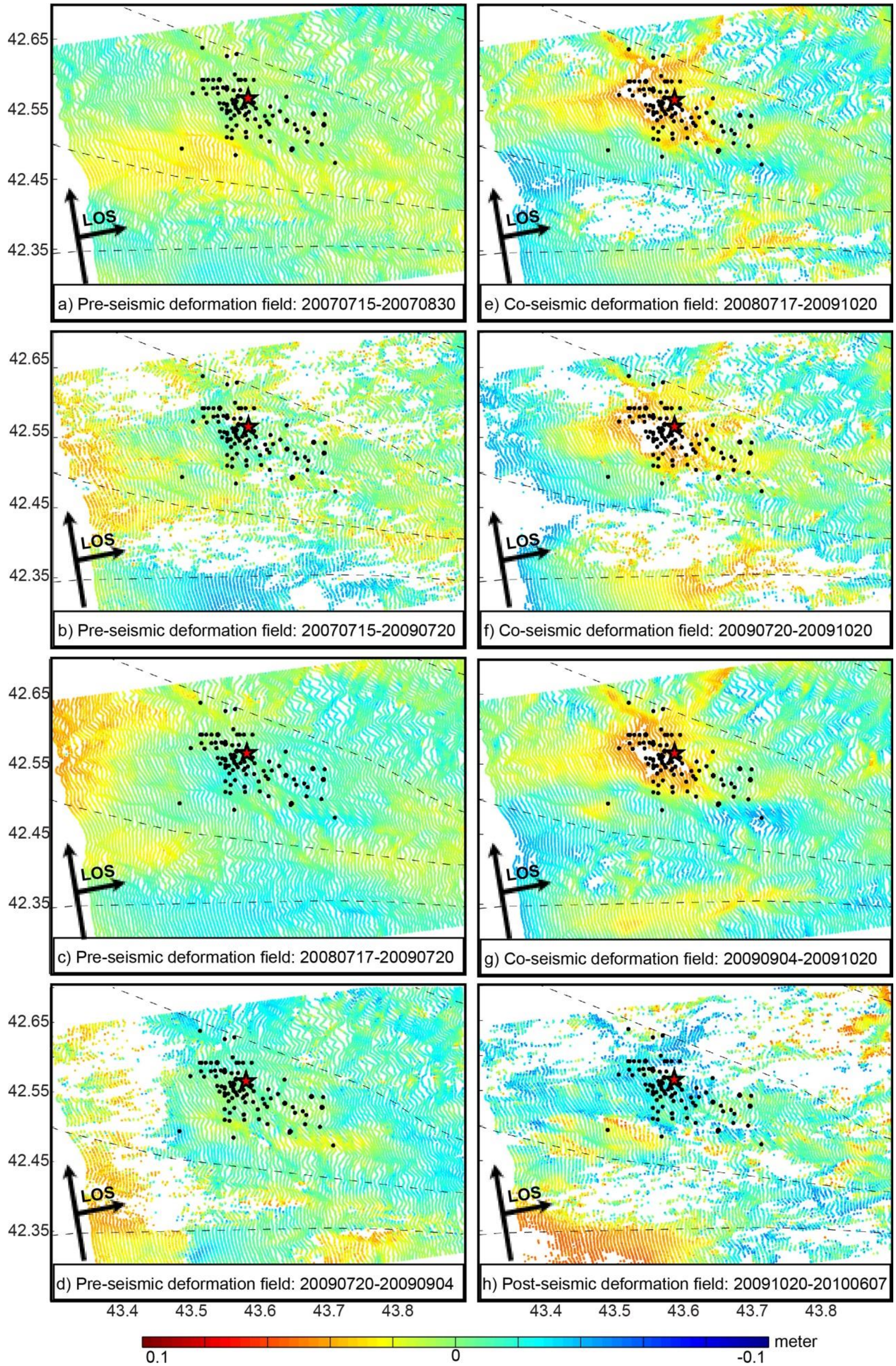

a) Pre-seismic deformation field: 20070715-20070830
b) Pre-seismic deformation field: 20070715-20090720
c) Pre-seismic deformation field: 20080717-20090720
d) Pre-seismic deformation field: 20090720-20090904
e) Co-seismic deformation field: 20080717-20091020
f) Co-seismic deformation field: 20090720-20091020
g) Co-seismic deformation field: 20090904-20091020
h) Post-seismic deformation field: 20091020-20100607
LOS
42.65
42.55
42.45
42.35
43.4
43.5
43.6
43.7
43.8
meter
0.1
0
-0.1

Figure 2. (a-d) Pre-seismic, (e-g) co-seismic and (h) post-seismic deformation fields. The star is the location of the main shock 2009. The black dots are the epicenters of the aftershocks from 2009 with magnitudes greater than 4 (from the catalog of the Seismic Monitoring Center (SMC) in Georgia, www.seismo.ge). Major faults are shown by black dashed lines (Gamkrelidze & Shengelia, 2007). Red colors represent movement toward the ascending satellite.

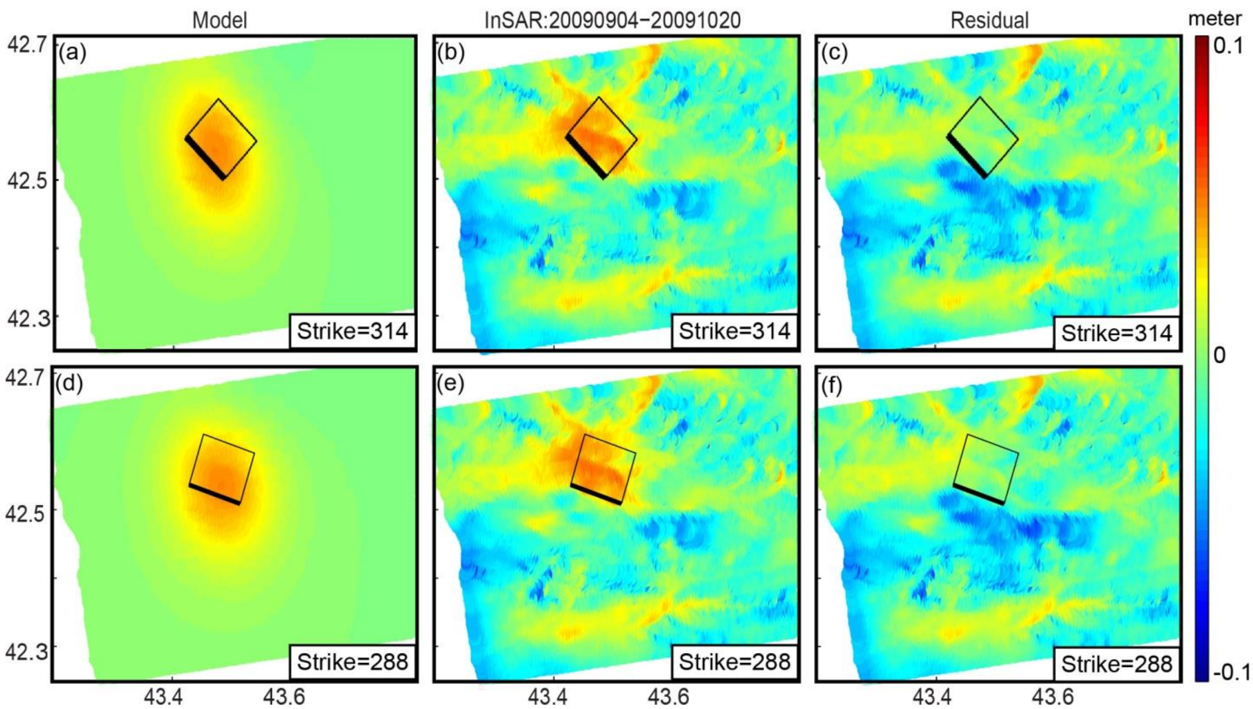

Figure 3. Pleriminary results of our forward modeling. (a) Model based on the CMT solution, (b) InSAR interferogram and (c) residual (right) between the observations and model. (d) Same as in the previous case, but with a different strike value, (e) InSAR interferogram and (f) residual between the observations and model . The black frames show the projection of fault plane.

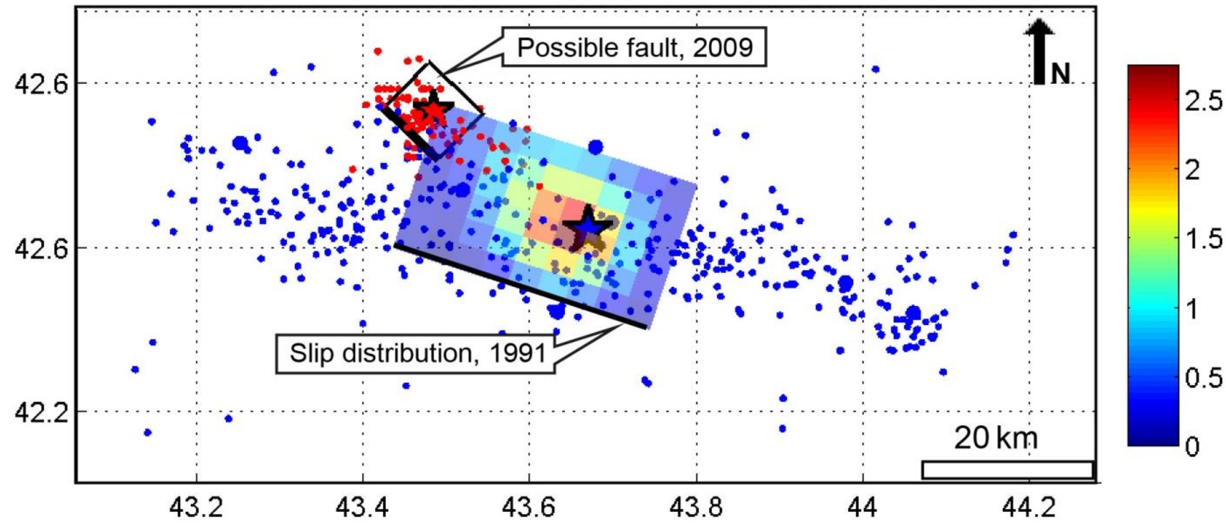

Figure 4. Surface projection of the co-seismic slip distribution of Tan and Taymaz (2006) for the 1991 earthquake. The blue dots are the aftershocks (M>3) and main shock (blue star) of the earthquake to the Mw=6.9 from seismic monitoring center (SMC) in Georgia catalog. The red dots represent the aftershocks located by SMC from the time of the earthquake to the Mw=6 (red star) event of September 7, 2009. The black frame presents the possible fault plane for the 2009 earthquake, calculated with Okada code based on the CMT solution. Bold lines show the edge of planes close to the surface.

Appendix

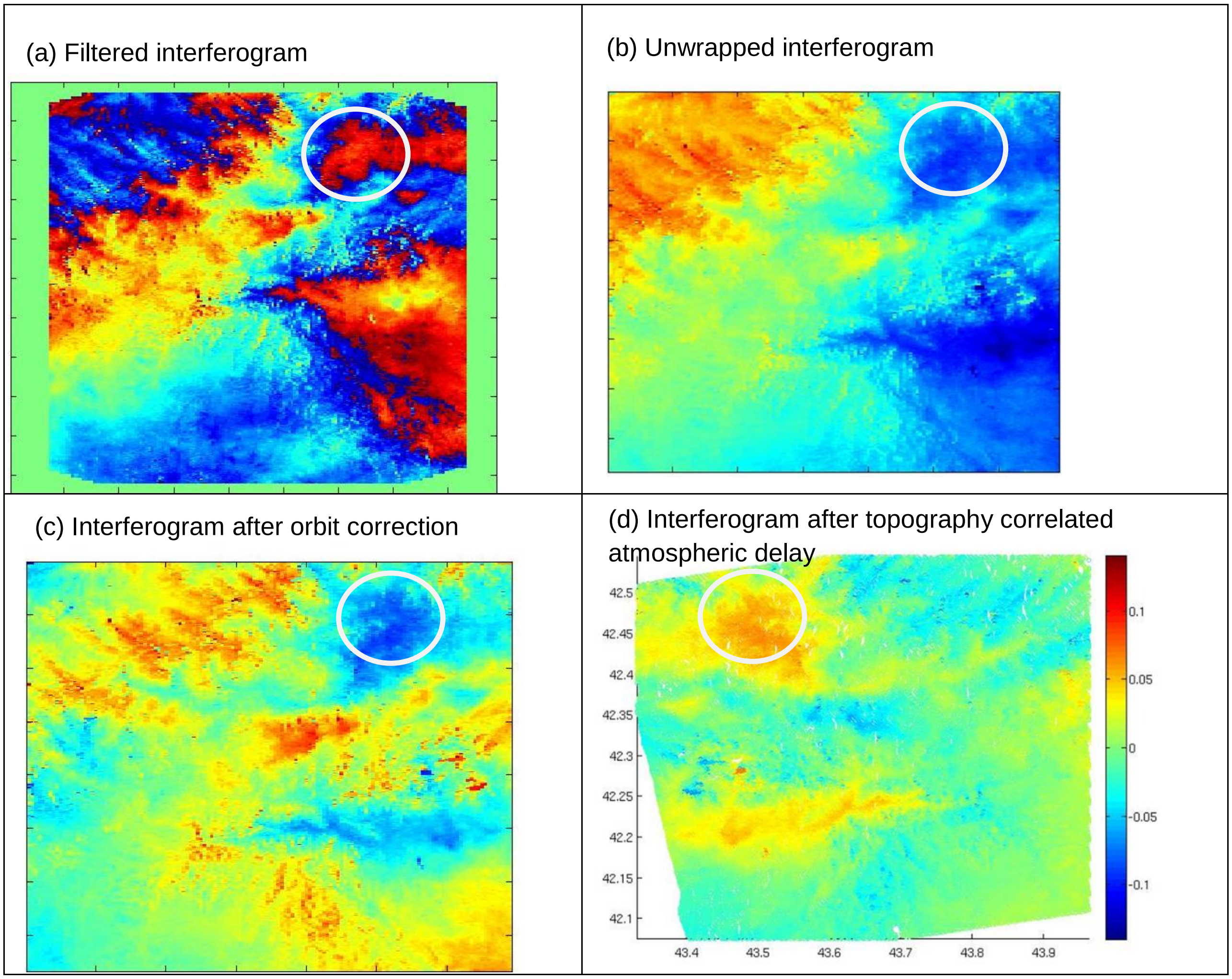

Figure. Example of the 20090904-20091020 interferogram processing stages: a,b,c in satellite azimuth-range coordinates; d in ground coordinates (UTM). The deformation signal is in the white circle.